catalysts

MDPI

Review

Review on Copper and Palladium Based Catalysts for Methanol Steam Reforming to Produce Hydrogen

Xinhai Xu [1,*], Kaipeng Shuai [1] and Ben Xu [2]

[1] School of Mechanical Engineering and Automation, Harbin Institute of Technology, Shenzhen Graduate School, Shenzhen 518055, China; kaipengshuai@foxmail.com

[2] Department of Mechanical Engineering, University of Texas Rio Grande Valley, Edinburg, TX 78539, USA; ben.xu@utrgv.edu

* Correspondence: xuxinhai@hit.edu.cn; Tel.: +86-755-86102680

Academic Editors: Benoît Louis, Qiang Wang and Marcelo Maciel Pereira
Received: 4 May 2017; Accepted: 26 May 2017; Published: 8 June 2017

Abstract: Methanol steam reforming is a promising technology for producing hydrogen for onboard fuel cell applications. The methanol conversion rate and the contents of hydrogen, carbon monoxide and carbon dioxide in the reformate, significantly depend on the reforming catalyst. Copper-based catalysts and palladium-based catalysts can effectively convert methanol into hydrogen and carbon dioxide. Copper and palladium-based catalysts with different formulations and compositions have been thoroughly investigated in the literature. This work summarized the development of the two groups of catalysts for methanol steam reforming. Interactions between the activity components and the supports as well as the effects of different promoters were discussed. Compositional and morphological characteristics, along with the methanol steam reforming performances of different Cu/ZnO and Pd/ZnO catalysts promoted by Al_2O_3, CeO_2, ZrO_2 or other metal oxides, were reviewed and compared. Moreover, the reaction mechanism of methanol steam reforming over the copper based and palladium based catalysts were discussed.

Keywords: copper based catalysts; palladium based catalysts; methanol steam reforming; hydrogen

1. Introduction

Hydrogen is a promising alternative fuel because of its high energy density and low greenhouse gas emission rate [1]. As an energy carrier, hydrogen can be used to produce electrical power in a fuel cell. The use of fuel cells is attractive for the vehicle industry due to their high energy conversion efficiency and low emissions [2]. However, refueling of hydrogen is a major obstacle for the deployment of fuel cell vehicles owing to the lack of infrastructure [3]. Onboard hydrogen production by a processing system which converts liquid hydrocarbon fuels into hydrogen is a practical solution [4,5]. Among various fuels, methanol receives attention for onboard processing applications because: (a) It is easy to handle and store; (b) It can be extracted from renewable sources and it is biodegradable; (c) Its reforming temperature is relatively low compared to the other fuels; and (d) Its tendency to form coke during reforming is low due to the high H/C ratio [6,7].

Three main onboard fuel processing mechanisms to produce hydrogen are steam reforming, partial oxidation and auto thermal reforming [8]. Steam reforming is the most industrial kind of mature technology and it is also the most commonly employed process to produce hydrogen from methanol reforming [9]. Among all the three mechanisms, steam reforming has the highest ratio of hydrogen and carbon monoxide in the reformate.

The performance of a methanol steam reforming process significantly depends on the catalyst. Ni-based catalysts are mostly used in large scale industrial processes. However, only around 20% of the catalysts can be effectively utilized in industrial processes [10]. Thereafter, excess amounts of catalysts

need to be used to counterbalance the effect of the low catalyst-utilization rate. For onboard methanol steam reforming, both the mass and size of the catalyst are restricted. Thus catalysts with higher activity and a better utilization rate are investigated. Interactions between the metal components and the support materials are critical for catalyst performance [11]. Promoters such as alkaline metals or acidic oxides are also important because they could promote the reactions following expected paths and help remove undesired matters that are formed during the reactions such as the carbonate species. Deactivation mechanisms including sintering and coke formation are also important concerns [12]. Overall, the objective for the development of an effective catalyst is to achieve the highest activity and hydrogen selectivity while minimizing the activity for side reactions such as methanol decomposition and maintaining the longest possible durability [9]. For different catalyst formulations, the influence of interactions between the catalyst components and the support as well as the addition of promoters on the structural, morphological and redox properties of the active phase needs to be examined.

The present work summarized the development of copper-based catalysts and palladium-based catalysts for methanol steam reforming. Interactions between the activity components and the supports as well as the effects of different promoters were discussed in detail. Methanol steam reforming performances based on different catalysts and the reaction mechanism were also presented. Besides copper-based and palladium-based catalysts, other metals such as nickel and cobalt are also used in catalysts for methanol steam reforming. Ni-based catalysts supported on alumina, zirconia, ceria and those containing Zn-Al or Mg-Al were intensively investigated for ethanol steam reforming instead of methanol reforming. The control of metallic Ni particle size and shape, as well as the redox properties of the catalyst system, are key factors in the preparation of Ni-based catalysts. Co and NiCo catalysts supported on cerium, lanthanum, zinc oxides, alumina and lantana-alumina were also studied for ethanol steam reforming. The key factors of Co-based catalysts are the control of metal morphology properties and the redox state of the system. A recent review summarized the progress of Ni-based and Co-based catalysts for methanol steam reforming [9]. Therefore they are not discussed in the present study.

2. Catalysts

2.1. Copper-Based Catalysts

Cu-based catalysts are commonly employed in methanol steam reforming reactions for onboard applications. Cu/ZnO catalysts are originally designed for methanol synthesis, and are also often used for methanol steam reforming because of the high activity at low operating temperature in the range of 250 °C and 300 °C. However, they need pre-treatment in hydrogen to obtain full activity, which is not convenient in small scale onboard systems [13]. Other disadvantages of the Cu/ZnO catalysts include the possibility of pyrophoric behavior occurring when exposed to air and the high sensitivity to a few ppm of sulfur [14].

Although it is confirmed that zinc leads to an improvement in the desired properties of the Cu/ZnO catalysts, the mechanism of the promotion effect of zinc is not completely understood [15]. Empirical experience indicates a particularly large Cu-ZnO contact is desired in order to improve the catalyst performance, whereas the casualty of the contact on the catalyst is still ambiguous [16]. Several different explanations of the mechanism can be found in the literature such as the spillover model, the metallic copper model and the Cu-Zn alloy model. The two-way transfer of hydrogen between Cu and ZnO is supposed to be crucial in the ZnO-promoted Cu system as explained in the spillover model [17]. Because ZnO has a large capacity for adsorbed hydrogen [18], it may trap H atoms originally produced on the Cu surface and serve as a reservoir to facilitate hydrogen spillover in the catalyst system. However, the hydrogen spillover from Cu to ZnO was found to be rapid from a partially oxidized Cu surface but limited from a fully reduced Cu surface [17]. In the metallic copper model, Cu particles supported on ZnO are confirmed in the metallic state by extended X-ray absorption fine-structure spectroscopy (EXAFS) [19]. However, the morphology of the Cu particle

may reversibly change under different operating gaseous conditions, while no detectable change of the ZnO phase can be observed. An increase of the oxidation potential in the operating gas can lead to more spherical Cu particles with larger particle size. In contrast, flat dish-like Cu particles can be obtained when the operating gaseous condition is reduced as shown in Figure 1a [20,21]. The metallic copper model also argues that Cu-Zn alloy may play a role in the Cu/ZnO system, but Cu-Zn alloy is only formed at extreme reducing operating conditions. However, the Cu-Zn alloy model claims that the role of ZnO in the Cu/ZnO system is not to support Cu but to separate Cu particles from sintering as a spacer. Thus the Cu/ZnO catalyst is a mixed system of Cu and ZnO particles as shown in Figure 1b. The Cu-Zn or Cu-O-Zn surface alloy is supposed to be responsible for the promotion effect of ZnO depending on the reaction conditions and the amount of Zn [22]. Activity of the Cu/ZnO catalyst was proposed to be related to the copper metal surface area. Alejo et al. [23] found that the catalyst $Cu_{40}Zn_{60}$ (containing Cu 40 wt.% and Zn 60 wt.%) showed the highest copper area in the series of Cu-Zn contents with copper relative content of 20–70 wt.%. Correspondingly, $Cu_{40}Zn_{60}$ has the highest activity for methanol reforming to produce hydrogen. Therefore it can be confirmed that the Cu-ZnO interaction also depends on the catalyst compositions. Both the turnover frequencies (TOF) and apparent activation energy change with the catalyst compositions.

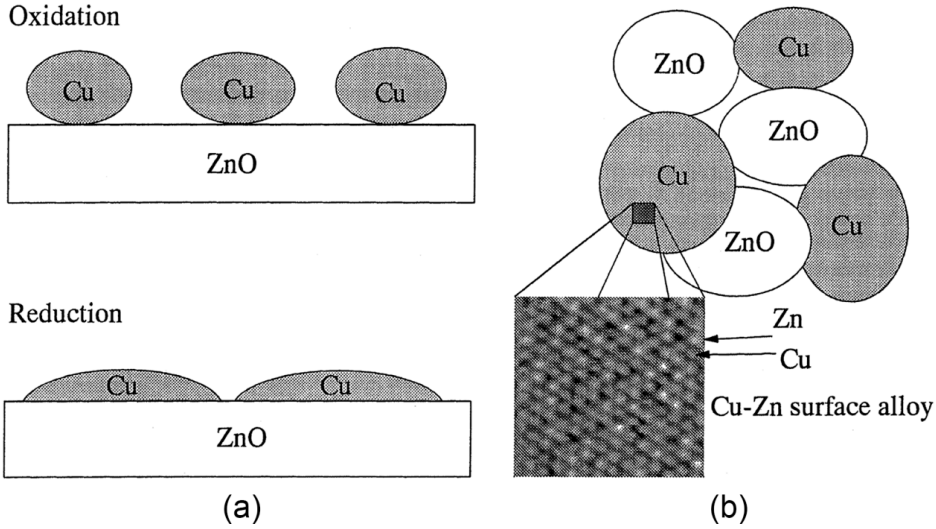

Figure 1. (**a**) The metallic copper model; and (**b**) The Cu-Zn alloy model (Adapted from [22], Copyright 2003, Springer).

Lunkenbein et al. [24] were the first to report clear evidence for the formation of metastable graphite-like (GL) ZnO layers in industrial $Cu/ZnO/Al_2O_3$ catalysts induced by strong metal-support interactions. High-angle annular dark field scanning transmission electron microscopy (HAADF-STEM) was employed to analyze the microstructure of the fresh catalyst in the reduced state. The results show that the Cu nanoparticles (in pink color) are homogeneously dispersed within a porous ZnO (in yellow color) rod-like matrix as shown in Figure 2. High resolution TEM results also indicate that the ZnO layer is 1 to 2 nm thick comprising four to six sheets with interlayer distance between 1.8 and 2.8 Å. The proposed scheme of Cu and ZnO interaction is shown in Figure 3. Although the TEM imaging shows almost complete surface coverage of Cu particles, the accessibility of the Cu surface is still unclear due to the fact that only 2D projections are indicated in TEM imaging. Fichtl et al. [25] concluded that about 30% of the Cu surface area is accessible based on H_2-temperature programed reduction (H_2-TPD) results. Lunkenbein et al. [24] argued that these results discredit the direct correlation between catalyst activity and surface area.

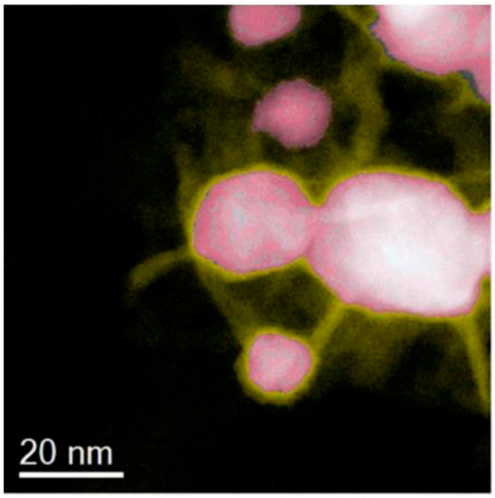

Figure 2. High-angle annular dark field scanning transmission electron microscopy (HAADF-STEM) image of $Cu/ZnO/Al_2O_3$ fresh catalyst (Adapted from [24], Copyright 2015, Wiley-VCH).

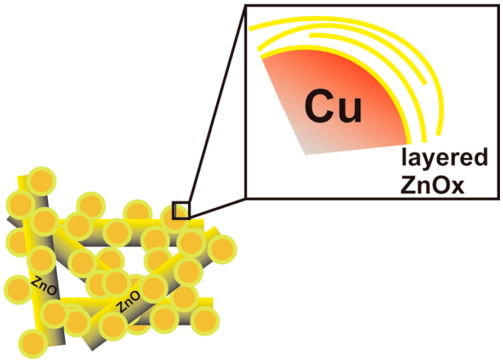

Figure 3. Illustration of $Cu/ZnO/Al_2O_3$ fresh catalyst after reduction (Adapted from [24], Copyright 2015, Wiley-VCH).

Stabilizers and promoters are often employed in Cu/ZnO catalysts. Alumina can be added as support of Cu-ZnO to increase the catalyst durability and selectivity of H_2 in the reformate [9]. Alejo et al. [23] found that the presence of alumina in $Cu_{40}Zn_{55}Al_5$ (containing Cu 40 wt.%, Zn 55 wt.% and Al 5 wt.%) had a slightly inhibiting effect on methanol conversion, whereas it significantly improved the catalyst stability and selectivity for H_2 and CO_2 with only traces of CO existing in the reformate. Without the addition of alumina, the $Cu_{40}Zn_{60}$ catalyst started to deactivate after 20 h at 503 K. In comparison, the durability of $Cu_{40}Zn_{55}Al_5$ was increased to more than 110 h at the same operating temperature [23]. A recent work reported that a Cu-Al spinel oxide catalyst can improve the activity for methanol steam reforming compared to the commercial $Cu/ZnO/Al_2O_3$ catalyst [26]. The Cu-Al spinel oxide catalysts can be used for methanol reforming without pre-reduction by H_2, which not only avoids the copper sintering prior to the reaction, but also slows down the sintering rate during reaction. The small amount of CuO phase in the catalyst can initiate the reforming reaction at a low temperature, and Cu can be released gradually from $CuAl_2O_4$ to sustain the reaction after initiation. Moreover, the activity of the Cu-Al spinel catalyst can be further improved by adding excess amount of Al_2O_3, which can increase the surface area and $CuAl_2O_4$ crystal dispersion [26].

Other alkaline oxides such as CeO_2 and ZrO_2 can also be added into the Cu-based catalysts as promoters. The addition of ceria oxide is beneficial for maintaining copper dispersion and coke suppression due to its oxygen storage property [27]. Cu/CeO_2 catalysts have been proven to have superior activities for steam methanol reforming compared to industrial Cu/ZnO catalysts [28]. The addition of cerium to $Cu/ZnO/Al_2O_3$ catalysts can effectively improve the activity and hydrogen

selectivity. In any case, the content of CO in the reformate can be kept low due to the suppression of methanol decomposition and reverse water-gas shift reactions [29]. Men et al. [30] reported that the activities of $Cu/CeO_2/Al_2O_3$ catalysts were dependent on the loading of Cu. They found that while the molar ratio of Cu and Ce in the catalyst increases from 0.1 to 0.9, the catalytic activity monotonously decreases. They attributed this to the fact that copper disperses preferentially on the ceria surface at low copper loading and the aggregation of copper particles occurs at high copper loading. Thermal desorption spectroscopy (TDS) results indicate that the decrease of copper loading and increase of ceria loading can enhance the basicity of the catalyst [31]. The methanol steam reforming reaction was believed to occur at the Cu/CeO_2 interface and the proposed reaction mechanism is shown in Figure 4 [30,32]. It includes four steps to fulfill a catalysis cycle, which are the adsorption of methanol and water at the Cu/CeO_2 interface, followed by the surface reaction and the oxygen reverse spillover (the migration of surface oxygen from CeO_2 to Cu), and, finally, the regeneration of partially oxidized copper and oxygen vacancies. ZrO_2 added to Cu/ZnO catalysts can also enhance the copper dispersion on the catalyst surface and thus lead to higher activity [33,34]. Moreover, the introduction of ZrO_2 into Cu/ZnO improves the reducibility and stability of the catalysts [35].

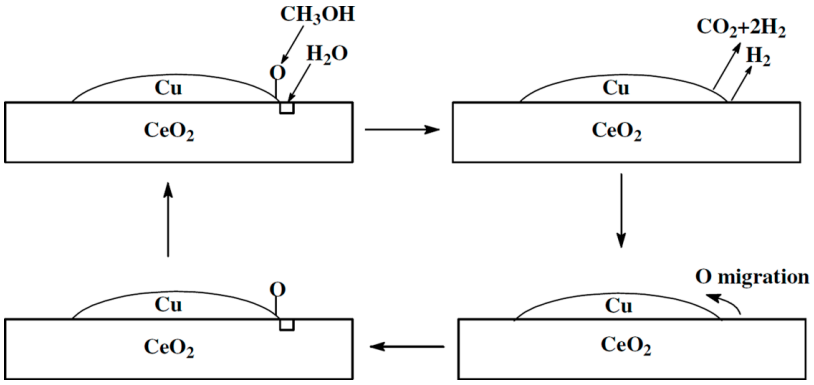

Figure 4. Proposed reaction mechanism of methanol steam reforming on $Cu/CeO_2/Al_2O_3$ catalyst (Adapted from [30], Copyright 2004, Elsevier).

2.2. Performances of Copper-Based Catalysts

Pan and Wang [36] experimentally tested a commercial $Cu/ZnO/Al_2O_3$ catalyst in a compact plate-fin reformer. The catalyst was grounded and sieved to the particle size of 0.442–0.681 mm before loading. The feeding reactants (CH_3OH and H_2O) flow rate was kept at a constant of 5 mL/min. Different molar ratios of H_2O and CH_3OH between 1.2 and 1.6 were examined. The results showed that the content of H_2 in the dry reformate was 74.5% regardless of the ratio of H_2O/CH_3OH, whereas the content of CO decreased from 1.0% to less than 0.5% as the ratio of H_2O/CH_3OH increased from 1.2 to 1.6. Thus, complete methanol conversion can be achieved in all the tests.

Zhang et al. [37,38] investigated the methanol steam reforming performances of the commercial Cu/ZnO, $Cu/ZnO/Al_2O_3$ (CB-7), $Cu/ZnO/CeO_2$, $Cu/ZnO/ZrO_2$, and $Cu/ZnO/CeO_2/ZrO_2$ catalysts. The experiments were conducted in a fixed-bed quartz tube reactor with the gas hourly space velocity (GHSV) of 1200 h^{-1}. The ratio of H_2O and CH_3OH in the reactants was kept at 1.2. At the reforming temperature of 250 °C, the methanol conversion is 97%, 97%, 80%, 75%, and 68% over $Cu/ZnO/ZrO_2$, $Cu/ZnO/CeO_2/ZrO_2$, $Cu/ZnO/CeO_2$, $Cu/ZnO/Al_2O_3$, and Cu/ZnO catalysts, respectively. The corresponding CO concentration in the dry reformate is 0.8%, 0.55%, 0.25%, 1.8%, and 0.3%, respectively. The results also show that no noticeable deactivation was observed during a 360 h continuous operation over the $Cu/ZnO/CeO_2/ZrO_2$ catalyst.

Baneshi et al. [39] compared the methanol steam reforming performances over $Cu/CeO_2/Al_2O_3$, $Cu/ZrO_2/Al_2O_3$, and $Cu/CeO_2/ZrO_2/Al_2O_3$ catalysts. The catalysts were evaluated in a fixed bed reactor with a constant GHSV of 10,000 cm^3 h^{-1}/g-catalyst. The ratio of H_2O and CH_3OH in the

reactant flow was kept at 1.5. At the reforming temperature of 240 °C, the methanol conversion is 100%, 95% and 94% over the $Cu/CeO_2/Al_2O_3$, $Cu/CeO_2/ZrO_2/Al_2O_3$, and $Cu/ZrO_2/Al_2O_3$ catalysts, respectively. For $Cu/CeO_2/Al_2O_3$, the H_2 content in the dry reformate is around 65% and only a trace amount of CO is detectable. In a long run test, the activity of $Cu/CeO_2/Al_2O_3$ remains at 100% after 110 h of continuous operation.

Zeng et al. [40] examined the $Cu/ZnO/ZrO_2/Al_2O_3$ catalyst in cube-post micro reactors. The catalyst was prepared by co-precipitation method and coated in the plate by the wash coating method. The fed reactant mixture had a flow rate varying from 2 to 6 mL/h. The ratio of H_2O and CH_3OH was 1.3. The results indicate that the highest methanol conversion of 70.27% was achieved at 280 °C. The H_2 concentration in the reformate were around 74.4%, and the CO concentration was about 1%. The low methanol conversion in this study resulted from the microreactor structure. With optimized microchannel structure and dimensions, the methanol conversion can be improved to around 95% [41].

Jones et al. [42] studied the performance of a $Cu/ZnO/ZrO_2/Al_2O_3$ catalyst containing ZrO_2 from a monoclinic nanoparticle ZrO_2 precursor instead of a $Zr(NO_3)_2$ precursor. The catalyst was prepared by the co-impregnation method and its compositions were 15 wt.% CuO-15 wt.% ZnO-10 wt.% ZrO_2-60 wt.% Al_2O_3. The total reactants fed rate was 0.8 mL/h and the ratio of H_2O and CH_3OH was 3. At 305 °C, the methanol conversation rate can achieve 80%, and the corresponding H_2 content in the dry reformate is almost 80%. Only a trace amount of CO exists in the reformate.

Chang et al. [43] compared the oxidative steam reforming of methanol performances over the $Cu/ZnO/ZrO_2/Al_2O_3$ catalyst and the commercial $Cu/ZnO/Al_2O_3$ catalyst. The $Cu/ZnO/ZrO_2/Al_2O_3$ catalyst was prepared by the co-precipitation method. Under the reaction conditions of fed rate = 3.5 mL/h, H_2O/CH_3OH = 1.1, O_2/CH_3OH = 0.1, temperature = 250 °C, $Cu/ZnO/ZrO_2/Al_2O_3$ (20/50/20/10 wt.%) shows higher activity than the commercial $Cu/ZnO/Al_2O_3$ (30/60/10 wt.%) catalyst. Methanol conversion rates are 75.3% and 65.5% over the two catalysts, respectively.

Ahmadi et al. [44] investigated the nanostructured $CuO/ZnO/ZrO_2/Al_2O_3$ catalyst synthesized by the sonochemically-assisted co-precipitation method using different ultrasonic power. BET results show that higher ultrasonic power results in higher surface area and better activity. When the catalyst is synthesized and assisted by 90 W ultrasonic power, it can achieve 100% methanol conversion at a relatively low temperature of 200 °C. The H_2 and CO concentrations in the dry reformate is above 75% and below 1%, respectively. No deactivation is observed after continuously running for 24 h.

2.3. Palladium Based Catalysts

Iwasa et al. [45] first experimentally tested Pd/ZnO, Pd/Al_2O_3, and Pd/ZrO_2 catalysts for methanol steam reforming. The results show that the catalyst characteristics were greatly affected by the support. For catalysts with 1.0 wt.% Pd loading, Pd/ZrO_2 has higher dispersion (28.9%) than Pd/ZnO (10.7%) and Pd/Al_2O_3 (13.1%). However, the TOF is the higher for Pd/ZnO (0.829 s^{-1}) compared to Pd/ZrO_2 (0.148 s^{-1}) and Pd/Al_2O_3 (0.152 s^{-1}). Pd/ZnO also has the highest selectivity for the steam reforming reaction of methanol. Only Pd/Al_2O_3 gave dimethyl ether in addition to hydrogen, carbon dioxide and carbon monoxide in the reformate.

Further investigation concludes that the catalytic performance of Pd/ZnO for methanol steam reforming can be greatly improved by reducing the catalyst prior to the reaction. Iwasa et al. [46] proposed that the Pd-Zn alloy formed in hydrogen treatment has positive effects on the selectivity of methanol steam reforming. Formaldehyde species formed in the reaction were able to be effectively transformed into H_2 and CO_2 over the catalyst containing Pd-Zn alloys. In contrast, the formaldehyde species selectively decomposed to H_2 and CO over metallic-palladium-dominated catalysts without reducing treatment.

Chin et al. [47] confirmed the formation of the Pd-Zn alloy in the reduced Pd/ZnO catalyst by XRD, TPR and TEM characterization techniques. Figure 5 shows the high resolution TEM graph of a

spent 16.7 wt.% Pd/ZnO catalyst. The presence of the Pd-Zn alloy was verified by the distinct d-lines of the small crystallites. It can also be concluded that Pd and Zn formed a highly ordered crystallites structure because the d-lines are continuous over an extended area as shown in Figure 5.

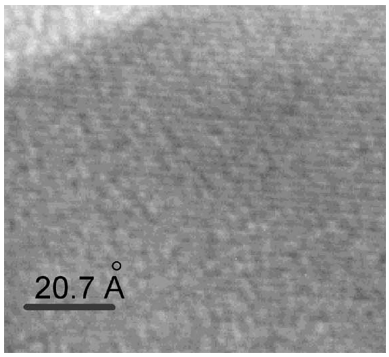

Figure 5. High resolution TEM graph of a spent 16.7 wt.% Pd/ZnO catalyst (Adapted from [47], Copyright 2002, Elsevier).

Chin et al. [48] also studied the effects of the preparation and pretreatment procedures on the Pd/ZnO catalyst. Using highly acidic Pd nitrate aqueous precursors such as the $Pd(NO_3)_2$ solution can alter the textural properties of the ZnO support including porosities and crystalline structures. The dissolution of ZnO into Zn^{2+} influenced the extent of mixing between Zn^{2+} and Pd^{2+} in pretreatment. As mentioned earlier, the formation of the Pd-Zn alloy was verified in the reducing pretreatment. Karim et al. [49] reported that the high temperature pretreatment (>300 °C) not only completely transformed Pd to Pd-Zn alloy, but also lead to particle growth. It is necessary to eliminate the small particles (<2 nm) because they lower the CO_2 selectivity of the Pd/ZnO catalyst.

XRD characterization of the spent catalyst indicates that Pd-Zn crystallites are strongly dependent on Pd loading, as shown by the catalytic performance [50]. Surface concentration of the Pd-Zn alloy increases as the Pd loading increases, but larger Pd-Zn crystallites resulting from higher Pd loading also inhibit the further increase of the surface concentration of the Pd-Zn alloy. Excess amounts of Pd loading could decrease the catalyst activity and increase the CO content in the reformate [51]. Liu et al. [52] suggested that 5 wt.% Pd loading is appropriate with regard to the catalytic activity. However, Pfeifer et al. [53] reported that the catalyst with 10 wt.% Pd loading showed the highest activity. Liu et al. [54] also studied the deactivation mechanisms of the Pd/ZnO catalyst. Two major routes that caused deactivation are carbon deposited on the catalyst surface and surface oxidation of the Pd-Zn alloy.

Pd/ZnO supported on alumina was also investigated for methanol steam reforming [55]. The activity of Pd/ZnO catalysts can be greatly improved by supporting them on alumina, and the $Pd/ZnO/Al_2O_3$ catalysts show better stability than the commercial $Cu/ZnO/Al_2O_3$ catalysts [56]. Zn-modified Pd catalysts supported on CeO_2 also show high selectivity for methanol steam reforming. XRD results indicate the formation of the Pd-Zn alloy, as well as the complete disappearance of the metallic Pd after reduction [57]. Methanol steam reforming performances over Pd/ZnO and Pd/CeO_2 catalysts were compared. The results show that Pd/ZnO has a lower methanol conversion rate and higher CO_2 selectivity than the Pd/CeO_2 catalyst. The average TOF at 230 °C for Pd/ZnO and Pd/CeO_2 was $0.8 \pm 0.3\ s^{-1}$ and $0.4 \pm 0.2\ s^{-1}$, respectively. Pd/ZnO has a higher density of acidic sites while Pd/CeO_2 has a higher density of basic sites [58].

Except for Zn, the catalytic functions of the Pd/Al_2O_3 and Pd/CeO_2 catalysts can be greatly modified by the addition of some other metals such as In and Ga due to the formation of Pd-In and Pd-Ga alloys [59–61]. Similarly to the Pd/ZnO catalysts, the alloys are responsible for the high CO_2 selectivity and the metallic Pd is responsible for CO selectivity. The ratios of Pd and the second metal as well as the loadings on the support have significant effects on the catalyst activity [62,63].

Pd/ZrO_2 catalysts were found to have high CO selectivity of approximately 50% at the reforming temperature of 260 °C [64,65]. Azenha et al. [64] first investigated the effect of Cu as a promoter of Pd/ZrO_2 catalysts. The results show that the addition of Cu into Pd supported on ZrO_2 with monoclinic crystalline structure leads to a remarkable decrease of the CO selectivity from 50% to 5%. SEM images shown in Figure 6 indicate the Cu and Pd particles are in intimate contact and highly dispersed in the support. The superior methanol steam reforming performance of the Cu-Pd/ZrO_2 catalyst is due to the strong interaction between Pd and Cu as well as the enhanced dispersion of the metal phase on the support.

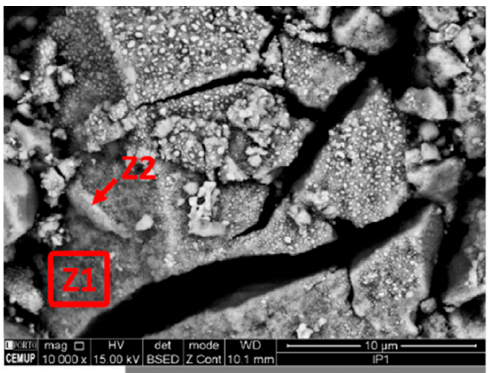

	Atomic weight (%)		
	Cu	**Pd**	**Zr**
Z1	8.2	1.1	22.5
Z2	12.7	2.1	24.4

Figure 6. SEM images of the $CuPd/ZrO_2$ catalyst with EDX quantification (Adapted from [64], Copyright 2017, Elsevier).

2.4. Performances of Palladium Based Catalysts

Echave et al. [66] experimentally examined the methanol steam reforming performance of the 2.5 wt.% Pd/ZnO catalyst. The catalyst was prepared by incipient wetness impregnation of pre-synthesized ZnO with a palladium nitrate solution. The catalyst was evaluated at the reforming temperature of 350 °C with a reactant flow rate of 0.064 mL/min and a steam to carbon ratio of 1.5. No obvious deactivation was observed during a 4000 min continuous operation. Methanol conversion higher than 90% can be reached. H_2 and CO contents in the dry reformate are 70% and less than 1%, respectively. Sanz et al. [67] washcoated 2.5 wt.% Pd/ZnO catalyst in microchannel reformers, and similar results were reported.

Xia et al. [68] investigated the methanol steam reforming performance over a series of $Pd/ZnO/Al_2O_3$ catalysts. Under the reforming conditions of 220 °C, GHSV = 14,400 h^{-1}, and H_2O/CH_3OH = 1.78, the methanol conversion is 14.3% and 46.5% over Pd/ZnO (Pd loading 8.6 wt.%) and $Pd/ZnO/Al_2O_3$ (Pd loading 8.9 wt.%), respectively. Both catalysts achieve CO_2 selectivity higher than 99%. While elevating the reforming temperature to 270 °C, 100% methanol conversion is reached over the $Pd/ZnO/Al_2O_3$ catalyst. Pd loading and the Pd/Zn ratio were also varied and the performances were compared with respect to the methanol conversion and CO_2 selectivity. The results showed that the catalyst with a Pd loading of 8.9 wt.% and a Pd/Zn ratio of 0.38 had the highest methanol conversion and CO_2 selectivity. At the reforming temperature of 250 °C, 80% methanol conversion can be obtained over this catalyst.

Barrios et al. [69] tested the performances of Pd/CeO_2 and $Pd/ZnO/CeO_2$ catalysts for methanol steam reforming. Pd/CeO_2 can only decompose methanol to CO at the reforming temperature of 250 °C and the steam to carbon ratio of 1. The methanol steam reforming reaction only occurs at the presence of zinc oxide. At 300 °C, the methanol conversion rate is 65% and 95% over Pd/ZnO and $Pd/ZnO/CeO_2$

catalysts, respectively. Although the $Pd/ZnO/CeO_2$ catalyst significantly improves the methanol conversion compared to Pd/ZnO, its CO_2 selectivity (80%) is lower than that of Pd/ZnO (90%).

Men et al. [62] studied the methanol steam reforming performance of Pd-In/Al_2O_3 catalysts with different Pd loadings and Pd/In ratios. The results show that the catalyst with 7.5 wt.% Pd and 10 wt.% In_2O_3 has the overall best performance considering both the methanol conversion rate and the CO content in the reformate. About 90% methanol conversion and 0.6% CO concentration are achieved at the reforming temperature of 375 °C, with total flow rate of 30 mL/min and a steam to carbon ratio of 1.5.

Kuc et al. [70] experimentally investigated methanol steam reforming over perovskite-type oxides catalysts of $LaCo_{0.87}Pd_{0.13}O_{3\pm\delta}$ (denoted as LCPO) and $LaCo_{0.85}Pd_{0.075}Zn_{0.075}O_{3\pm\delta}$ (denoted as LCPZO). At the reforming temperature of 250 °C, with a total flow rate of 100 mL/min and a H_2O to CH_3OH ratio of 1.3, the methanol conversion rate is about 90% and 30% for LCPO and LCPZO, respectively. The corresponding CO_2 selectivity is 10% and 60%, respectively.

2.5. Reaction Mechanism of Methanol Steam Reforming

Regarding the reaction mechanism of methanol steam reforming over copper-based catalysts, four schemes have been proposed [7] including a methanol decomposition-water gas shift reaction scheme [71], a 1-step methanol steam reforming scheme [72,73], a methanol steam reforming-methanol decomposition-reverse water gas shift reaction scheme [74,75] and a methyl formate scheme [76–78]. The methanol steam reforming-methanol decomposition-reverse water gas shift reaction scheme is also adopted for methanol steam reforming over palladium catalysts [79,80].

The reaction scheme proposed by Peppley et al. [74,75] claimed the three reactions of methanol decomposition, water gas shift reaction, and methanol steam reforming all occur in parallel. This scheme has been supported and experimentally validated by different researchers [81–87]. The three parallel reactions are shown in Equations (1)–(3).

$$CH_3OH + H_2O \underset{k_{-1}}{\overset{k_1}{\leftrightarrow}} 3H_2 + CO_2 \quad (1)$$

$$CO_2 + H_2 \underset{k_{-2}}{\overset{k_2}{\leftrightarrow}} H_2O + CO \quad (2)$$

$$CH_3OH \overset{k_3}{\rightarrow} 2H_2 + CO \quad (3)$$

As indicated above, both the methanol steam reforming and reverse water gas shift reactions are reversible, and the methanol decomposition reaction is irreversible. k_1, k_2 and k_3 are the forward rate constants, while k_{-1} and k_{-2} are the backward rate constants.

Mastalir et al. [82] evaluated the reaction rate coefficients of the above three reactions. The Arrhenius equations are shown in Equations (4)–(6).

$$r_1 = k_1 C_{CH_3OH}^{0.6} C_{H_2O}^{0.4} \exp\left(-\frac{E_{a1}}{RT}\right) - k_{-1} C_{CO_2} C_{H_2} \exp\left(-\frac{E_{a1}}{RT}\right) \quad (4)$$

$$r_2 = k_2 C_{CO_2} C_{H_2} \exp\left(-\frac{E_{a2}}{RT}\right) - k_{-2} C_{CO} C_{H_2O} \exp\left(-\frac{E_{a2}}{RT}\right) \quad (5)$$

$$r_3 = k_3 C_{CH_3OH}^{1.3} \exp\left(-\frac{E_{a3}}{RT}\right) \quad (6)$$

Chein et al. [88] proposed a different model including the methanol steam reforming reaction, methanol decomposition reaction and water gas shift reaction as shown in Equations (7)–(9). All the reactions are assumed to be irreversible.

$$CH_3OH + H_2O \rightarrow 3H_2 + CO_2 \quad (7)$$

$$CH_3OH \rightarrow 2H_2 + CO \tag{8}$$

$$H_2O + CO \rightarrow CO_2 + H_2 \tag{9}$$

Semi-empirical kinetic models proposed by Suh et al. [89] were used for the methanol steam reforming and decomposition reactions, which are,

$$r_R = (1-\varepsilon)\rho_s k_R C_{CH_3OH} \tag{10}$$

$$r_D = (1-\varepsilon)\rho_s k_D \tag{11}$$

where C is the molar concentration, ε is the catalyst layer porosity, and ρ_s is the catalyst density. The rate constants k_R and k_D can be expressed as,

$$k_R = 5.5\left(1.15 \times 10^6 + 9.41 \times 10^5 \ln \varphi\right) e^{-E_R/RT} \tag{12}$$

$$k_D = 5.5 \times 7.09 \times 10^7 e^{-E_D/RT} \tag{13}$$

where φ is the molar ratio of water to methanol, and E_R and E_D are the activation energies of the reforming and decomposition reactions, respectively.

Studies of Purnama et al. [90] and Chen et al. [91] were used for the water gas shift reaction. The reaction rate is expressed as,

$$r_{WGS} = 11.2 k_{WGS}\left(p_{CO} p_{H_2O} - p_{CO_2} p_{H_2}/\mathrm{K_{eq}}\right) \tag{14}$$

$$k_{WGS} = 1.78 \times 10^{22}\left(1 - 0.154\delta + 0.008\delta^2\right) T^8 e^{-E_{WGS}/RT} \tag{15}$$

$$\mathrm{K_{eq}} = \exp\left(\frac{4577.8}{T} - 4.33\right) \tag{16}$$

where k_{WGS} and K_{eq} are the rate constant and the equilibrium constant of the water gas shift reaction, respectively. p is the partial pressure of a species, and δ is the molar ratio of water to carbon monoxide.

3. Conclusions

Methanol steam reforming is a promising technology to produce hydrogen-rich syngas with only a trace amount of carbon monoxide for onboard fuel cell applications. The performance of methanol steam reforming is significantly dependent on the reforming catalyst. The present work reviewed the commonly used copper-based and palladium-based catalysts for methanol steam reforming. Compositional and morphological characteristics, along with the methanol steam reforming performances of the two groups of catalysts were summarized.

Concerning the copper-based catalysts, it is confirmed that the Cu/ZnO catalysts have high activity towards methanol steam reforming reactions. However, the mechanism of the promotion effect of zinc oxide is still under discussion. One widely accepted theory is that Cu-Zn alloys formed in the Cu/ZnO catalysts are responsible for the promotion effect of ZnO. Alumina can be added to the Cu/ZnO catalysts as a stabilizer to increase the durability and selectivity of hydrogen, although it slightly reduces the methanol conversion rate. Other alkaline oxides such as CeO_2 and ZrO_2 can also be added as promoters. The addition of ceria oxide is beneficial for maintaining copper dispersion and coke suppression. The catalytic activity and hydrogen selectivity of the Cu/ZnO catalysts are also enhanced by the addition of ceria oxide. The introduction of ZrO_2 into Cu/ZnO improves the reducibility and stability of the catalysts.

As for the palladium-based catalysts, the Pd/ZnO catalysts were found to have similar activities with the copper-based catalysts for methanol steam reforming. Moreover, they have higher carbon dioxide selectivity due to the formation of Pd-Zn alloys. The Pd-Zn crystallites and the catalytic performance of the catalysts are both strongly affected by the loading of Pd. An optimum range of Pd

loading between 5% and 10% exists as reported in the literature. The activity of Pd/ZnO catalysts can be greatly improved by supporting them on alumina, and the $Pd/ZnO/Al_2O_3$ catalysts show better stability than the commercial $Cu/ZnO/Al_2O_3$ catalysts.

Several schemes have been proposed regarding the reaction mechanism of methanol steam reforming. The methanol steam reforming-methanol decomposition-reverse water gas shift reaction scheme is generally accepted for methanol steam reforming reactions occurring over the copper-based or palladium-based catalysts. In this scheme, the three reactions of the methanol decomposition, water gas shift reaction and methanol steam reforming are assumed to occur in parallel. Two different models based on this scheme were also presented in this work.

Acknowledgments: Support from Shenzhen Science and Technology Research and Development Funds (JCYJ20160318094917454) and Harbin Institute of Technology is gratefully acknowledged.

Author Contributions: All authors contributed to write the paper.

Conflicts of Interest: The authors declare no conflict of interest.

References

1. Zhang, S.; Wang, X.; Xu, X.; Li, P. Hydrogen production via catalytic autothermal reforming of desulfurized Jet—A fuel. *Int. J. Hydrog. Energy* **2017**, *42*, 1932–1941. [CrossRef]
2. Aicher, T.; Lenz, B.; Gschnell, F.; Groos, U.; Federici, F.; Caprile, L.; Parodi, L. Fuel processors for fuel cell APU applications. *J. Power Sources* **2006**, *154*, 503–508. [CrossRef]
3. Xu, X.; Zhang, S.; Li, P. Autothermal reforming of n-dodecane and desulfurized Jet-A fuel for producing hydrogen-rich syngas. *Int. J. Hydrog. Energy* **2014**, *39*, 19593–19602. [CrossRef]
4. Choudhury, A.; Chandra, H.; Arora, A. Application of solid oxide fuel cell technology for power generation—A review. *Renew. Sustain. Energy Rev.* **2013**, *20*, 430–442. [CrossRef]
5. Xu, X.; Zhang, S.; Wang, X.; Li, P. Fuel adaptability study of a lab-scale 2.5 kWth autothermal reformer. *Int. J. Hydrog. Energy* **2015**, *40*, 6798–6808. [CrossRef]
6. Iulianelli, A.; Ribeirinha, P.; Mendes, A.; Basile, A. Methanol steam reforming for hydrogen generation via conventional and membrane reactors: A review. *Renew. Sustain. Energy Rev.* **2014**, *29*, 355–368. [CrossRef]
7. Yong, C.; Ooi, C.; Chai, S.; Wu, X. Review of methanol reforming-Cu-based catalysts, surface reaction mechanisms, and reaction schemes. *Int. J. Hydrog. Energy* **2013**, *38*, 9541–9552. [CrossRef]
8. Xu, X.; Liu, X.; Xu, B. A survey of nickel-based catalysts and monolithic reformers of the onboard fuel reforming system for fuel cell APU applications. *Int. J. Energy Res.* **2016**, *40*, 1157–1177. [CrossRef]
9. Kubacka, A.; Fernandez-Garcia, M.; Martinez-Arias, A. Catalytic hydrogen production through WGS or steam reforming of alcohols over Cu, Ni and Co catalysts. *Appl. Catal. A* **2016**, *518*, 2–17. [CrossRef]
10. Christensen, T. Adiabatic prereforming of hydrocarbons—An important step in syngas production. *Appl. Catal. A* **1996**, *138*, 285–309. [CrossRef]
11. Kubacka, A.; Martines-Arias, A.; Fernandez-Garcia, M. Role of the interface in base-metal ceria-based catalysts for hydrogen purification and production processes. *ChemCatChem* **2015**, *7*, 3614–3624. [CrossRef]
12. Alenazey, F.; Cooper, C.; Dave, C.; Elnashaie, S.; Susu, A.; Adesina, A. Coke removal from deactivated Co–Ni steam reforming catalyst using different gasifying agents: An analysis of the gas–solid reaction kinetics. *Catal. Commun.* **2009**, *10*, 406–411. [CrossRef]
13. Kolb, G. Review: Microstructured reactors for distributed and renewable production of fuels and electrical energy. *Chem. Eng. Process.* **2013**, *65*, 1–44. [CrossRef]
14. Lindstrom, B.; Petterson, L. Deactivation of copper-based catalysts for fuel cell applications. *Catal. Lett.* **2001**, *74*, 27–30. [CrossRef]
15. Rameshan, C.; Stadlmayr, W.; Penner, S.; Lorenz, H.; Memmel, N.; Havecker, M.; Blume, R.; Teschner, D.; Rocha, T.; Zemlyanov, D.; et al. Hydrogen production by methanol steam reforming on copper boosted by zinc-assisted water activation. *Angew. Chem. Int. Ed.* **2012**, *51*, 3002–3006. [CrossRef] [PubMed]
16. Kasatkin, I.; Kurr, P.; Kniep, B.; Trunschke, A.; Schlogl, R. Role of lattice strain and defects in copper particles on the activity of Cu/ZnO/Al2O3 catalysts for methanol synthesis. *Angew. Chem. Int. Ed.* **2007**, *119*, 7465–7468. [CrossRef]

17. Burch, R.; Golunski, E.; Spencer, M. The role of copper and zinc oxide in methanol synthesis catalysts. *J. Chem. Soc. Faraday Trans.* **1990**, *86*, 2683–2691. [CrossRef]
18. Bowker, M.; Hadden, R.; Houghton, H.; Hyland, J.; Waugh, K. The mechanism of methanol synthesis on copper/zinc oxide/alumina catalysts. *J. Catal.* **1988**, *109*, 263–273. [CrossRef]
19. Clausen, B.; Schiøtz, J.; Gråbæk, L.; Ovesen, C.; Jacobsen, K.; Nørskov, J.; Topsøe, H. Wetting/non-wetting phenomena during catalysis: Evidence from in situ on-line EXAFS studies of Cu-based catalysts. *Top. Catal.* **1994**, *1*, 367–376. [CrossRef]
20. Grunwaldt, J.D.; Molenbroek, A.; Topsoe, N.Y.; Topsoe, H.; Clausen, B. In Situ investigations of structural changes in Cu/ZnO catalysts. *J. Catal.* **2000**, *194*, 452–460. [CrossRef]
21. Yurieva, T.; Plyasova, L.; Makarova, O.; Krieger, T. Mechanisms for hydrogenation of acetone to isopropanol and of carbon oxides to methanol over copper-containing oxide catalysts. *J. Mol. Catal.* **1996**, *113*, 455–468. [CrossRef]
22. Nakamura, J.; Choi, Y.; Fujitani, T. On the issue of the active site and the role of ZnO in Cu/ZnO methanol synthesis catalysts. *Top. Catal.* **2003**, *22*, 277–285. [CrossRef]
23. Alejo, L.; Lago, R.; Pena, M.; Fierro, J. Partial oxidation of methanol to produce hydrogen over Cu-Zn-based catalysts. *Appl. Catal. A* **1997**, *162*, 281–297. [CrossRef]
24. Lunkenbein, T.; Schumann, J.; Behrens, M.; Schlogl, R.; Willinger, M. Formation of a ZnO overlayers in industrial Cu/ZnO/Al2O3 catalysts induced by strong metal-support interactions. *Angew. Chem. Int. Ed.* **2015**, *54*, 4544–4548. [CrossRef] [PubMed]
25. Fichtl, M.; Schumann, J.; Kasatkin, I.; Jacobsen, N.; Behrens, M.; Schlogl, R.; Muhler, M.; Hinrichsen, O. Counting of oxygen defects versus metal surface sites in methanol synthesis catalysts by different probe molecules. *Angew. Chem. Int. Ed.* **2014**, *53*, 7043–7047. [CrossRef] [PubMed]
26. Xi, H.; Hou, X.; Liu, Y.; Qing, S.; Gao, Z. Cu-Al spinel oxide as an efficient catalyst for methanol steam reforming. *Angew. Chem. Int. Ed.* **2014**, *53*, 11886–11889. [CrossRef] [PubMed]
27. Gao, J.; Guo, J.; Liang, D.; Hou, Z.; Fei, J.; Zheng, X. Production of syngas via autothermal reforming of methane in a fluidized-bed reactor over the combined CeO_2-ZrO_2/SiO_2 supported Ni catalysts. *Int. J. Hydrog. Energy* **2008**, *33*, 5493–5500. [CrossRef]
28. Liu, Y.; Hayakawa, T.; Suzuki, K.; Hamakawa, S. Production of hydrogen by steam reforming of methanol over Cu/CeO_2 catalysts derived from $Ce_{1-x}Cu_xO_{2-x}$ precursors. *Catal. Commun.* **2001**, *2*, 195–200. [CrossRef]
29. Patel, S.; Pant, K. Activity and stability enhancement of copper-alumina catalysts using cerium and zinc promoters for the selective production of hydrogen via steam reforming of methanol. *J. Power Sources* **2006**, *159*, 139–143. [CrossRef]
30. Men, Y.; Gnaser, H.; Zapf, R.; Hessel, V.; Ziegler, C. Parallel screening of Cu/CeO_2/γ-Al_2O_3 catalysts for steam reforming of methanol in a 10-channel micro-structured reactor. *Catal. Commun.* **2004**, *5*, 671–675. [CrossRef]
31. Men, Y.; Gnaser, H.; Ziegler, C.; Zapf, R.; Hessel, V.; Kolb, G. Characterization of Cu/CeO_2/γ-Al_2O_3 thin film catalysts by thermal desorption spectroscopy. *Catal. Lett.* **2005**, *105*, 35–40. [CrossRef]
32. Men, Y.; Gnaser, H.; Zapf, R.; Hessel, V.; Ziegler, C.; Kolb, G. Steam reforming of methanol over Cu/CeO_2/γ-Al_2O_3 catalysts in a microchannel reactor. *Appl. Catal. A* **2004**, *277*, 83–90. [CrossRef]
33. Wu, G.; Mao, D.; Lu, G.; Cao, Y.; Fan, K. The role of the promoters in Cu based catalysts for methanol steam reforming. *Catal. Lett.* **2009**, *130*, 177–184. [CrossRef]
34. Jeong, H.; Kim, K.; Kim, T.; Ko, C.; Park, H.; Song, I. Hydrogen production by steam reforming of methanol in a micro-channel reactor coated with Cu/ZnO/ZrO_2/Al_2O_3 catalyst. *J. Power Sources* **2006**, *159*, 1296–1299. [CrossRef]
35. Huang, G.; Liaw, B.; Jhang, C.; Chen, Y. Steam reforming of methanol over CuO/ZnO/CeO_2/ZrO_2/Al_2O_3 catalysts. *Appl. Catal. A* **2009**, *358*, 7–12. [CrossRef]
36. Pan, L.; Wang, S. Modeling of a compact plate-fin reformer for methanol steam reforming in fuel cell systems. *Chem. Eng. J.* **2005**, *108*, 51–58. [CrossRef]
37. Zhang, L.; Pan, L.; Ni, C.; Sun, T.; Zhao, S.; Wang, S.; Wang, A.; Hu, Y. CeO_2-ZrO_2-promoted CuO/ZnO catalyst for methanol steam reforming. *Int. J. Hydrog. Energy* **2013**, *38*, 4397–4406. [CrossRef]

38. Zhang, L.; Pan, L.; Ni, C.; Sun, T.; Wang, S.; Hu, Y.; Wang, A.; Zhao, S. Effects of precipitation aging time on the performance of CuO/ZnO/CeO_2-ZrO_2 for methanol steam reforming. *J. Fuel Chem. Technol.* **2013**, *41*, 883–888. [CrossRef]
39. Baneshi, J.; Haghighi, M.; Jodeiri, N.; Abdollahifar, M.; Ajamein, H. Homogeneous precipitation synthesis of CuO-ZrO_2-CeO_2-Al_2O_3 nanocatalyst used in hydrogen production via methanol steam reforming for fuel cell applications. *Energy Convers. Manag.* **2014**, *87*, 928–937. [CrossRef]
40. Zeng, D.; Pan, M.; Wang, L.; Tang, Y. Fabrication and characteristics of cube-post microreactors for methanol steam reforming. *Appl. Energy* **2012**, *91*, 208–213. [CrossRef]
41. Pan, M.; Wu, Q.; Jiang, L.; Zeng, D. Effect of microchannel structure on the reaction performance of methanol steam reforming. *Appl. Energy* **2015**, *154*, 416–427. [CrossRef]
42. Jones, S.; Neal, L.; Everett, M.; Hoflund, G.; Hagelin-Weaver, H. Characterization of ZrO_2-promoted Cu/ZnO/nano-Al_2O_3 methanol steam reforming catalysts. *Appl. Surf. Sci.* **2010**, *256*, 7345–7353. [CrossRef]
43. Chang, C.; Chang, C.; Chiang, S.; Liaw, B.; Chen, Y. Oxidative steam reforming of methanol over CuO/ZnO/CeO_2/ZrO_2/Al_2O_3 catalysts. *Int. J. Hydrog. Energy* **2010**, *35*, 7675–7683. [CrossRef]
44. Ahmadi, F.; Haghighi, M.; Ajamein, H. Sonochemically coprecipitation synthesis of CuO/ZnO/ZrO_2/Al_2O_3 nanocatalyst for fuel cell grade hydrogen production via steam methanol reforming. *J. Mol. Catal. A* **2016**, *421*, 196–208. [CrossRef]
45. Iwasa, N.; Kudo, S.; Takahashi, H.; Masuda, S.; Takezawa, N. Highly selective supported Pd catalysts for steam reforming of methanol. *Catal. Lett.* **1993**, *19*, 211–216. [CrossRef]
46. Iwasa, N.; Masuda, S.; Ogawa, N.; Takezawa, N. Steam reforming of methanol over Pd/ZnO: Effect of the formation of PdZn alloys upon the reaction. *Appl. Catal. A* **1995**, *125*, 145–157. [CrossRef]
47. Chin, Y.; Dagle, R.; Hu, J.; Dohnalkova, A.; Wang, Y. Steam reforming of methanol over highly active Pd/ZnO catalyst. *Catal. Today* **2002**, *77*, 79–88. [CrossRef]
48. Chin, Y.; Wang, Y.; Dagle, R.; Li, X. Methanol steam reforming over Pd/ZnO: Catalyst preparation and pretreatment studies. *Fuel Process Technol.* **2003**, *83*, 193–201. [CrossRef]
49. Karim, A.; Conant, T.; Datye, A. The role of PdZn alloy formation and particle size on the selectivity for steam reforming of methanol. *J. Catal.* **2006**, *243*, 420–427. [CrossRef]
50. Zhang, H.; Sun, J.; Dagle, V.; Halevi, B.; Datye, A.; Wang, Y. Influence of ZnO facets on Pd/ZnO catalysts for methanol steam reforming. *ACS Catal.* **2014**, *4*, 2379–2386. [CrossRef]
51. Liu, S.; Takahashi, K.; Uematsu, K.; Ayabe, M. Hydrogen production by oxidative methanol reforming on Pd/ZnO. *Appl. Catal. A* **2005**, *283*, 125–135. [CrossRef]
52. Liu, S.; Takahashi, K.; Ayabe, M. Hydrogen production by oxidative methanol reforming on Pd/ZnO catalyst: Effects of Pd loading. *Catal. Today* **2003**, *87*, 247–253. [CrossRef]
53. Pfeifer, P.; Schubert, K.; Liauw, M.; Emig, G. PdZn catalysts prepared by washcoating microstructured reactors. *Appl. Catal. A* **2004**, *270*, 165–175. [CrossRef]
54. Liu, S.; Takahashi, K.; Fuchigami, K.; Uematsu, K. Hydrogen production by oxidative methanol reforming on Pd/ZnO: Catalyst deactivation. *Appl. Catal. A* **2006**, *299*, 58–65. [CrossRef]
55. Ota, A.; Kunkes, E.; Kasatkin, I.; Groppo, E.; Ferri, D.; Poceiro, B.; Yerga, R.; Behrens, M. Comparative study of hydrotalcite-derived supported Pd2Ga and PdZn intermetallic nanoparticles as methanol synthesis and methanol steam reforming catalysts. *J. Catal.* **2012**, *293*, 27–38. [CrossRef]
56. Conant, T.; Karim, A.; Lebarbier, V.; Wang, Y.; Girgsdies, F.; Schlogl, R.; Datye, A. Stability of bimetallic Pd-Zn catalysts for the steam reforming of methanol. *J. Catal.* **2008**, *257*, 64–70. [CrossRef]
57. Iwasa, N.; Mayanagi, T.; Nomura, W.; Arai, M.; Takezawa, N. Effect of Zn addition to supported Pd catalysts in the steam reforming of methanol. *Appl. Catal. A* **2003**, *248*, 153–160. [CrossRef]
58. Ranganathan, E.; Bej, S.; Thompson, L. Methanol steam reforming over Pd/ZnO and Pd/CeO_2 catalysts. *Appl. Catal. A* **2005**, *289*, 153–162. [CrossRef]
59. Iwasa, N.; Takezawa, N. New supported Pd and Pt alloy catalysts for steam reforming and dehydrogenation of methanol. *Top. Catal.* **2003**, *22*, 215–224. [CrossRef]
60. Collins, S.; Delgado, J.; Mira, C.; Calvino, J.; Bernal, S.; Chiavassa, D.; Baltanas, M.; Bonivardi, A. The role of Pd-Ga bimetallic particles in the bifunctional mechanism of selective methanol synthesis via CO_2 hydrogenation on a Pd/Ga_2O_3 catalyst. *J. Catal.* **2012**, *292*, 90–98. [CrossRef]

61. Mayr, L.; Lorenz, H.; Armbruster, M.; Villaseca, S.; Luo, Y.; Cardoso, R.; Burkhardt, U.; Zemlyanov, D.; Haevecker, M.; Blume, R.; et al. The catalytic properties of thin film Pd-rich $GaPd_2$ in methanol steam reforming. *J. Catal.* **2014**, *309*, 231–240. [CrossRef]
62. Men, Y.; Kolb, G.; Zapf, R.; O'Connell, M.; Ziogas, A. Methanol steam reforming over bimetallic Pd-In/Al_2O_3 catalysts in a microstructured reactor. *Appl. Catal. A* **2010**, *380*, 15–20. [CrossRef]
63. Föttinger, K. The effect of CO on intermetallic PdZn/ZnO and Pd_2Ga/Ga_2O_3 methanol steam reforming catalysts: A comparative study. *Catal. Today* **2013**, *208*, 106–112. [CrossRef]
64. Azenha, C.; Mateos-Pedrero, C.; Queiros, S.; Concepcion, P.; Mendes, A. Innovative ZrO_2-supported CuPd catalysts for the selective production of hydrogen from methanol steam reforming. *Appl. Catal. B* **2017**, *203*, 400–407. [CrossRef]
65. Kopfle, N.; Mayr, L.; Schmidmair, D.; Bernardi, J.; Knop-Gericke, A.; Havecker, M.; Klotzer, B.; Penner, S. A Comparative Discussion of the Catalytic Activity and CO_2-Selectivity of Cu-Zr and Pd-Zr (Intermetallic) Compounds in Methanol Steam Reforming. *Catalysts* **2017**, *7*, 53. [CrossRef]
66. Echave, F.; Sanz, O.; Montes, M. Washcoating of micro-channel reactors with PdZnO catalyst for methanol steam reforming. *Appl. Catal. A* **2014**, *474*, 159–167. [CrossRef]
67. Sanz, O.; Velasco, I.; Reyero, I.; Legorburu, I.; Arzamendi, G.; Gandia, L.; Montes, M. Effect of the thermal conductivity of metallic monoliths on methanol steam reforming. *Catal. Today* **2016**, *273*, 131–139. [CrossRef]
68. Xia, G.; Holladay, J.; Dagle, R.; Jones, E.; Wang, Y. Development of highly active Pd-ZnO/Al_2O_3 catalysts for microscale fuel processor applications. *Chem. Eng. Technol.* **2005**, *28*, 515–519. [CrossRef]
69. Barrios, C.; Bosco, M.; Baltanas, M.; Bonivardi, A. Hydrogen production by methanol steam reforming: Catalytic performance of supported-Pd on zinc-cerium oxides' nanocomposites. *Appl. Catal. B* **2015**, *179*, 262–275. [CrossRef]
70. Kuc, J.; Weidenkaff, A.; Matam, S. Methanol steam reforming on perovskite-type oxides $LaCo_{1-x-y}Pd_xZn_yO_{3\pm\delta}$: Effect of Pd/Zn on CO_2 Selectivity. *Top. Catal.* **2015**, *58*, 905–909. [CrossRef]
71. Santacesaria, E.; Carra, S. Kinetics of a catalytic steam reforming of methanol in a CSTR reactor. *Appl. Catal.* **1983**, *5*, 345–358. [CrossRef]
72. Breen, J.; Meunier, F.; Ross, J. Mechanistic aspects of the steam reforming of methanol over a CuO/ZnO/ZrO_2/Al_2O_3 catalyst. *Chem. Commun.* **1999**, *22*, 2247–2248. [CrossRef]
73. Agrell, J.; Bigersson, H.; Boutonnet, M. Steam reforming of methanol over Cu/ZnO/Al_2O_3 catalysts: A kinetic analysis and trategies for suppression of CO formation. *J. Power Sources* **2002**, *106*, 249–257. [CrossRef]
74. Peppley, B.; Amphlett, J.; Kearns, L.; Mann, R. Methanol-steam reforming on Cu/ZnO/Al_2O_3. Part 1. The reaction network. *Appl. Catal. A* **1999**, *179*, 21–30. [CrossRef]
75. Peppley, B.; Amphlett, J.; Kearns, L.; Mann, R. Methanol-steam reforming on Cu/ZnO/Al_2O_3. Part 2. A comprehensive kinetic model. *Appl. Catal. A* **1999**, *179*, 31–49. [CrossRef]
76. Jiang, C.; Trimm, D.; Wainwright, M. Kinetic mechanism for the reaction between methanol and water over a Cu-ZnO-Al_2O_3 catalyst. *Appl. Catal. A* **1993**, *97*, 145–158. [CrossRef]
77. Jiang, C.; Trimm, D.; Wainwright, M. Kinetic study of stream reforming of methanol over copper-based catalysts. *Appl. Catal. A* **1993**, *93*, 245–255. [CrossRef]
78. Breen, J.; Ross, J. Methanol reforming for fuel-cell applications: Development of zirconia-containing Cu-Zn-Al catalysts. *Catal. Today* **1999**, *51*, 521–533. [CrossRef]
79. Cao, C.; Xia, G.; Holladay, J.; Jones, E.; Wang, Y. Kinetic studies of methanol steam reforming over Pd/ZnO catalyst using a microchannel reactor. *Appl. Catal. A* **2004**, *262*, 19–29. [CrossRef]
80. Uriz, I.; Arzamendi, G.; Dieguez, P.; Echave, F.; Sanz, O.; Montes, M.; Gandia, L. CFD analysis of the effects of the flow distribution and heat losses on the steam reforming of methanol in catalytic (Pd/ZnO) microreactors. *Chem. Eng. J.* **2014**, *238*, 37–44. [CrossRef]
81. Frank, B.; Jentoft, F.; Soerijanto, H.; Krohnert, J.; Schlogl, R.; Schomacker, R. Steam reforming of methanol over copper-containing catalysts: Influence of support material on microkinetics. *J. Catal.* **2007**, *246*, 177–192. [CrossRef]
82. Mastalir, A.; Frank, B.; Szizybalski, A.; Soerijanto, H.; Deshpande, A.; Niederberger, M.; Schomacker, R.; Schlogl, R.; Ressler, T. Steam reforming of methanol over Cu/ZrO_2/CeO_2 catalysts: A kinetic study. *J. Catal.* **2005**, *230*, 464–475. [CrossRef]

83. Harold, M.; Nair, B.; Kolios, G. Hydrogen generation in a Pd membrane fuel processor: Assessment of methanol-based reaction systems. *Chem. Eng. Sci.* **2003**, *58*, 2551–2571. [CrossRef]
84. Morillo, A.; Freund, A.; Merten, C. Concept and design of a novel compact reactor for autothermal steam reforming with integrated evaporation and CO cleanup. *Ind. Eng. Chem. Res.* **2004**, *43*, 4624–4634. [CrossRef]
85. Gallucci, F.; Paturzo, L.; Basile, A. Hydrogen recovery from methanol steam reforming in a dense membrane reactor: Simulation study. *Ind. Eng. Chem. Res.* **2004**, *43*, 2420–2432. [CrossRef]
86. Hsueh, C.; Chu, H.; Yan, W.; Leu, G.; Tsai, J. Three-dimensional analysis of a plate methanol steam micro-reformer and a methanol catalytic combustor with different flow channel designs. *Int. J. Hydrog. Energy* **2011**, *36*, 13575–13586. [CrossRef]
87. Tadbir, M.; Akbari, M. Methanol steam reforming in a planar wash coated microreactor integrated with a micro-combustor. *Int. J. Hydrog. Energy* **2011**, *36*, 12822–12832. [CrossRef]
88. Chein, R.; Chen, Y.; Chung, J. Thermal resistance effect on methanol-steam reforming performance in micro-scale reformers. *Int. J. Hydrog. Energy* **2012**, *37*, 250–262. [CrossRef]
89. Suh, J.; Lee, M.; Greif, R.; Grigoropoulos, C. A study of steam methanol reformer in a micro-reactor. *J. Power Sources* **2007**, *173*, 458–466. [CrossRef]
90. Purnama, H.; Ressler, T.; Jentoft, R.; Soerijanto, H.; Schlogl, R.; Schomacker, R. CO formation/selectivity for steam reforming of methanol with a commercial $CuO/ZnO/Al_2O_3$ catalysts. *Appl. Catal. A* **2004**, *259*, 83–94. [CrossRef]
91. Chen, W.; Lin, M.; Jiang, T.; Chen, M. Modeling and simulation of hydrogen generation from high temperature and low temperature water gas shift reactions. *Int. J. Hydrog. Energy* **2008**, *33*, 6644–6656. [CrossRef]